MACHİNİNG OF NİCKEL BASED SUPER ALLOY BASED ON THE TAGUCHİ METHOD

Abdullah ALTIN

Van Vocational School of Higher Education, Yuzuncu Yıl University, 65100 Van, Turkey, aaltin@yyu.edu.tr

Abstract

In this paper, were determined the effects of cutting tool coating material and cutting speed on cutting forces and surface roughness based on Taguchi experimental design method. Main cutting force, Fz is considered to be cutting force as a criterion. In the experiments, depending on the tool coating material, lowest main cutting force is found to be 548 N with KC9240 CVD coated cemented carbide and Lowest average surface roughness (0.812 μm) with KT313 uncoated cemented carbide insert both at 100 m/min. The effects of machining parameters were investigated using Taguchi L_{18} orthogonal array. Optimal cutting conditions were determined using the signal-to-noise (S/N) ratio which is calculated for average surface roughness and cutting force according to the "the smaller is better" approach. Using results of analysis of variance (ANOVA) and signal-to–noise (S/N) ratio, effects of parameters on both average surface roughness and cutting forces were statistically investigated. It has seen that while cutting speed and cutting tool has higher effect on the cutting force, the cutting tool and cutting speed has higher effect on average surface roughness. The results obtained indicated that CVD cutting tools performed better than PVD and uncoated cutting tools according to cutting forces, but in terms of surface quality was observed poor performance with KC 9240 and KT315 by current parameters.

Keywords: Machinability, Optimized by Taguchi design of experiments, Inconel 625, Surface roughness, Cutting force.

Nomenclature

v	cutting speed in m/min
f	feed in mm/tooth
da	axial depth in mm
y	tool life in min
Fm	feed in mm per min
TL	total length

1. INTRODUCTION

Inconel 625 has long been used in aqueous corrosive environments due to its excellent overall corrosion resistance [1]. Inconel 625 (Alloy 625) is a nickel-based superalloy strengthened mainly by the solid-solution hardening effect of the refractory metals, niobium and molybdenum, in a nickel–chromium matrix [2]. Alloy 625 was originally developed as a solid-solution strengthened material. It was soon determined that the alloy is somewhat precipitation (age) hardenable [3-6]. Inconel 625 exhibits precipitation hardening mainly due to the precipitation of fine metastable phase [Ni3Nb] after annealing over a long period in the temperature range 550–850 ◦C [4,5]. Moreover, various forms of carbides (MC,M6C and M23C6) can also precipitate depending upon the time and temperature of ageing. Alloy 625 has found extensive use in many industries for diverse applications over a wide temperature range from cryogenic conditions to ultra hot environments over 1000 ◦C [6-9]. The alloy is endowed with good combination of yield strength, creep strength, fatigue strength and excellent oxidation and corrosion resistance in aggressive environments. Moreover, its good

weldability and fabricability have made it the choice for many diverse applications. Thus, over 50 years, alloy 625 has been widely used in aerospace, chemical, petrochemical and marine applications. However, many of the Inconel 625 components are highly complex shapes that are very expensive to produce due to extensive machining [10,11]. Cutting forces and surface roughness are two important issues in the machining of Super alloys. In the last decades, different types of dynamometers have been used in industry and research laboratories for understanding the principles of chip formation [12], for developing cutting force models [13], as well as for cutting process control [14], tool geometry optimization [15], tool condition monitoring [16-19] and for detection and suppression of chatter vibrations [20-21]. Cutting forces have a direct influence on specific cutting pressure and power consumption, For this reason, a commercially available Kistler piezoelectric dynamometer have been used for cutting force monitoring during machining [22,23]. With the increasing demand for reduced product tool wear and heat generation. Surface roughness is an important characteristic that describes the quality of the machined surface being, in most cases, a technical requirement for machined products. In addition, the surface roughness affects several attributes of machined parts like friction, wear, and heat transmission [24].

2. MATERIALS AND METHOD

2.1 Experiment Specimens

Specimens of Inconel 625, which has an industrial usage, are prepared as the dimension of diameter Ø 2''x40'' then used for the experiments. The chemical composition and mechanical properties of specimens are given in Table 1 And Table 2 respectively.

Table 1 Chemical composition of Inconel 625 workpiece material

Ni	Cr	Mo	Fe	Co	Nb+Ta	Mn	Al	P	Ti	Si
58%	22%	9,1%	4,73%	0,08%	5,325%	0,11%	0,21%	0,015%	0,33%	0,1%

Table 2 Mechanical properties of Inconel 625

Hardness (RB)	Tensile strength (MPa)	Yield strength (MPa)	breaking extension (5do)	Thermal Conductivity (W/mK)	young's mod. E [GPa]
97	885	758	60-30	9,8	206

2.2 Machine Tool and Measuring Instrument of Cutting Forces

In the experimental study machining tests are carried out on JOHNFORD T35 industrial type CNC lathe max. power of which is 10 kW and has revolution number between 50 and 3500 rev/min. during dry cutting process, Kistler brand 9257 B-type three-component piezoelectric dynamometer under tool holder with the appropriate load amplifier is used for measuring three orthogonal cutting forces (F_x, F_y, F_z). This allows direct and continuous recording and simultaneous graphical visualization of the three cutting forces.

2.3 Cutting Parameters, Cutting Tool and Tool Holder

During cutting process, the machining tests were conducted with three different cemented carbide tools namely Physical Vapor Deposition (PVD) coated with layers of TiN/TiCN/TiN; Chemical Vapor Deposition (CVD) coated with layers of TİN+AL2O3-TİCN+TİN; and WC/CO respectively. The cutting speeds (5*0, 65, 80, and 100 m/min)* were chosen by taking into consideration of ISO 3685 standard as recommended by manufacturing companies. The depth of cut *(1,5 mm)* and feed rate *(0,10-0,15 mm/rev.)* were chosen

constant. The dimension of test specimens were chosen 2''x40'' in terms of diameter and long. Properties of cutting tools and level of independent variables are given in Table 3 and Table 4. Surtrasonic 3-P measuring equipment is used for the measurement of surface roughness. The inserts is mounted on PCLNR 2525 M12 type tool holders with 75° approaching.

Table 3 Properties of cutting tools

Coating material(top layer)	Coating method and layers	ISO grade of material (grade)	Geometric form	Manufacturer and code
TiN	CVD (TiN, AL2O3, TiCN TiN, Wc)	P25-P40, M20-M30	CNMG120412R	Kennametal KC9240
TiN	PVD (TiN, TiCN, TiN, Wc)	P25-P40, M20-M30	CNMG120412FN	Kennametal KT315
WC-CO	Uncoated	P25-P40, M20-M30	CNMG120412MS	Kennametal K313

Table 4 Level of independent variables

Variables	Level of variables			
	Lower	Low	Medium	High
Cutting force ,*v (m/min.)*	50	65	80	100
Feed rate, f (mm/rev.)	0,1-0,15	0,1-0,15	0,1-0,15	0,1-0,15
Depth of cut, (mm)	1,5	1,5	1,5	1,5

3 RESULTS AND DISCUSSION

3.1 The Change of Main Cutting Force Depending on Cutting Speed and Coating Material of Cutting Tool

After prepared test specimens were cut for experimental purposes, they were measured with a three-component piezoelectric dynamometer to obtain the main cutting force. According to Figure 1, increasing cutting speed decreases the main cutting force, excluding the area between 50 m/min and 80 m/min for K313. The obtained lowest main cutting force values at the cutting speeds of 50 m/min 577 N, 65 m/min 560 N, 80 m/min 550 N, and 100 m/min 548 N on 0,1 mm/rev. constant feed rate respectively. The lowest main cutting force is observed at 100 m/min cutting speed as 548 N. In Figure 1, the main cutting force depending on cutting speed and uncoating material of cutting tool were changed in all experiments. Decrement of cutting force depends on material type, working conditions and cutting speed range [25]. High temperature at flow region and decreasing contact area and chip thickness cause cutting force to decrease depending on cutting speed [25-27]. As widely known, cutting speed must be decreased to improve average surface roughness [25]. The scatter plot between surface roughness and cutting speed as shown in Figure 2, here indicated that there is linear relationship between surface roughness and cutting speed. The results of Figure 2 show that average surface roughness decreases 368% with increasing cutting speed from 50 m/min. to 100 m/min. by KC9240 (0,15 mm/rev. constant). The main cutting force decreases in spite of increasing the cutting speed from 50 to 100 m/min. As a result of experimental data, an increase of 100 % in cutting speed (from 50 to 100 m/min) , an increase has found in the main cutting force with K313 (0,01 %), a decrease with KT315 (0,015 %) and KC9240 (11%).

3.2 Optimization with the Taguchi Method

In this section, optimization of turning parameters was carried out in terms of cutting forces with the Taguchi analysis. The importance order of the effects of each control factor on turning forces was identified. For this purpose, the factors selected in the Taguchi experimental design and the levels of these factors are shown in Table 5. Taguchi's L18 2*1 3*2 mixed design was used. In the Taguchi method, there are three categories such as "the smallest is better", "The biggest is better" and "the nominal is better" for the calculation of the signal/noise (S/N) ratio. In the *i*th experiment, the S/N ratio _i can be calculated using the following equation [25].

$$\eta_i = -10 \log_{10} \qquad (1)$$

n is the number of replications and Yi is the measured characteristic.

3.3 Confirmation Experiments

Empirical relations between cutting forces and machining parameters are modelled in exponential form as follow:

$$e = c1(Fc)c2\ (Ff)c3\ (Fr)c4\ (L)c5\ (2) \qquad (2)$$

where **e** is the diametral error (_m), *c*1, *c*2, *c*3, *c*4 and *c*5 are constants, *F*c the main cutting (tangential) force, *F*f the feed (axial) force, *F*r the radial force (N) and *L* is the distance from the chuck (mm). The final step of the Taguchi experimental design process includes confirmation experiments [19,20]. For this aim, the results of the experiments were compared with the predicted values with the Taguchi method and the error rates were obtained. S/N ratios were predicted using the following model Moreover, the main cutting force or Fz were calculated using the following equation [21],

$$\eta predict = \eta m + \sum_{i=1}^{kn} (\eta i - \eta m) \qquad (3)$$

where *Y* predict is the main cutting force or Fz with regard to the S/N ratio.

$$Y_{predict} = 10^{\frac{-S/N}{20}} \qquad (4)$$

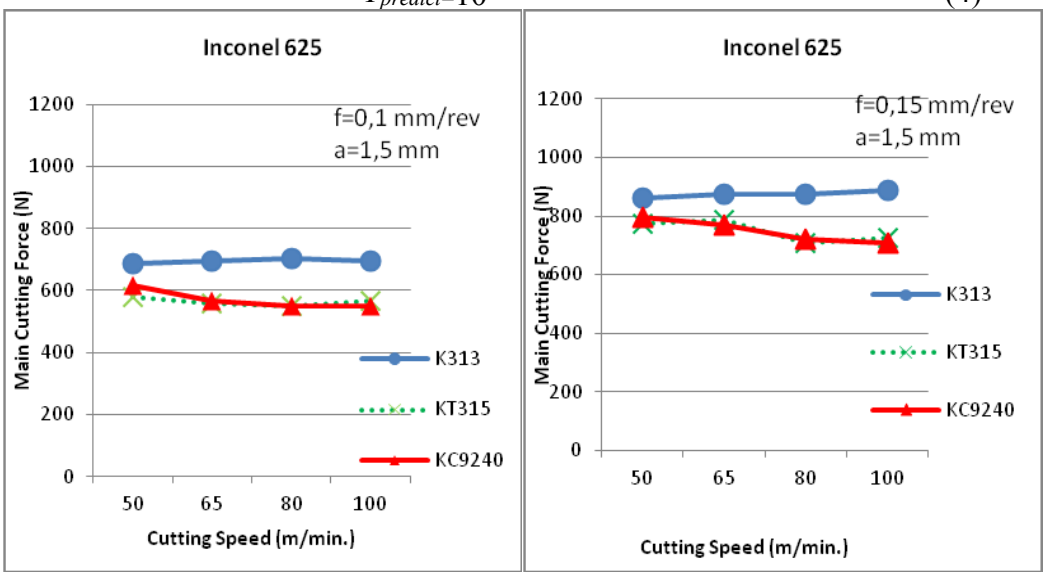

(a) (b)

Fig. 1 The change of main cutting force in Inconel 625 material according to cutting speed (a) At f=0,1 mm/rev. (b) At f=0,15 mm/rev.

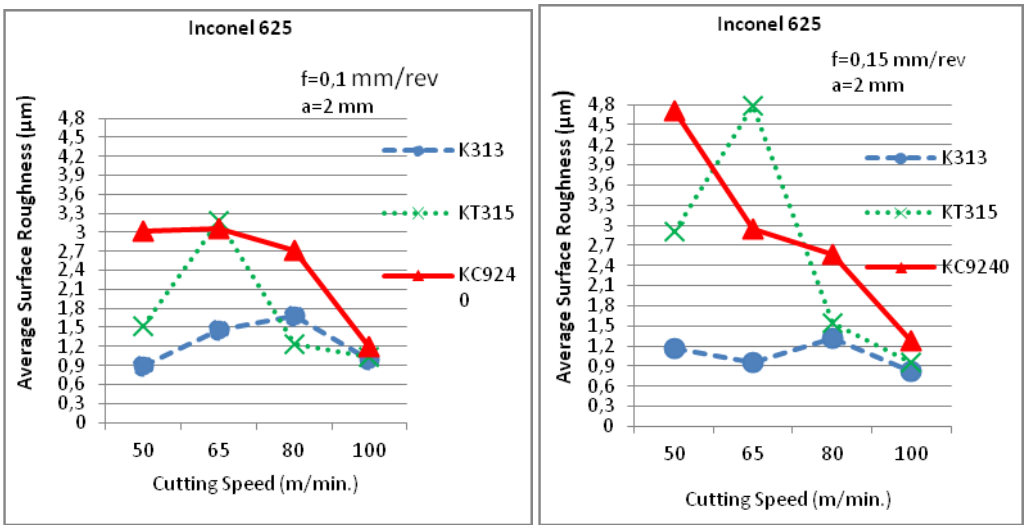

(a) (b)

Fig. 2 The change average surface roughness in Inconel 625 material according to cutting speed (a) At f=0,1 mm/rev. (b) At f=0,15 mm/rev.

where *Y* predict is the main cutting force or Fz with regard to the S/N ratio. Figure 3 and Figure 4 shows mean response graphs of the cutting forces and surface roughness respectivelly. Obtained results average surface roughness Ra, (µm) and main cutting force Fz (N) in the experiments and (S/N) ratios are shown in Table 6.

Table 5 Cutting parameters and levels

Control parameters		Units	Levels		
			1	2	3
Cutting speed (m/min.)	(A)	m/min.	65	80	100
Feed rate (mm/rev.)	(B)	(mm/rev.)	0,1	0,15	
Cutting tool	(C)		K313	KT315	KC9240

3.4 Taguchi Analysis: FZ versus Feed rate; Cutting Speed (m/min.); Cutting Tool

Linear Model Analysis: SN ratios versus Feed rate; Cutting Speed (m/min.); Cutting Tool

In Figure 2, it is observed, the effect of feed rate, cutting speed and cutting tool material on the average surface roughness clearly. According to this figure, in order to obtain the smallest surface roughness, it is necessary to use KT 313 cutting tool at low feed rate (0,10mm/rev.) and high cutting speed (100 m / min). According to **Table 7**, the effect of cutting tool on cutting force was obtained as 398 % and according to **Table 8**, the effect of cutting speed on average surface roughness was obtained 237 % as in high levels. Confirmation tables for cutting force and average surface roughness showed in **Table 9** and **Table 10** respectively.

Table 6 Obtained results average surface roughness Ra, (μm) and main cutting force Fz (N) in the experiments and S/N ratios.

Feedrate	Cutting speed	Cutting tool	Average surface roughness Ra(μm)	Main cutting force Fz (N)	S/N ratio For Ra	S/N ratio For Fz
0,10	65	K313	1,452	695	-3,2393	-56,8397
0,10	65	KT315	3,179	560	-10,0458	-54,9638
0,10	65	KC9240	0,725	505	2,7932	-54,0658
0,10	80	K313	1,691	705	-4,5629	-56,9638
0,10	80	KT315	1,235	550	-1,8333	-54,8073
0,10	80	KC9240	0,576	508	4,7916	-54,1173
0,10	100	K313	1,001	695	-0,0087	-56,8397
0,10	100	KT315	1,027	568	-0,2314	-55,0870
0,10	100	KC9240	0,755	483	2,4411	-53,6789
0,15	65	K313	0,958	875	0,3727	-58,8402
0,15	65	KT315	4,785	785	-13,5976	-57,8974
0,15	65	KC9240	1,580	691	-3,9731	-56,7896
0,15	80	K313	1.307	876	-62,3255	-58,8501
0,15	80	KT315	1,533	707	-3,7108	-56,9884
0,15	80	KC9240	1,476	555	-3,3817	-54,8859
0,15	100	K313	0.812	887	-58,1911	-58,9585
0,15	100	KT315	0,950	724	0,4455	-57,1948
0,15	100	KC9240	1,380	1,511	-2,7976	-63,5853

Table 7 ANOVA results for primary cutting force, F_z (for S/N ratios)

Source	Degrees of freedom (DoF)	Sequential sumof squares (SS)	Mean sum of squares (MS)	F-test	P-coefficient (%)
Cutting tool	1	39,388	39,388	11,51	0,398
Feed rate	2	6,631	3,316	0,97	0,067
Cutting speed	2	11,702	5,851	1,71	0,118
Residual error	12	41,063	3,422		0,415
Total	17	98,784			

Table 8. ANOVA results for surface roughness, Ra (μm) (for S/N ratios)

Source	Degrees of freedom (DoF)	Sequential sumof squares (SS)	Mean sum of squares (MS)	F-test	P-coefficient (%)
Cutting tool	1	1046,7	1046,74	3,49	0,165
Feed rate	2	165,4	82,72	0,28	0,026
Cutting speed	2	1498,3	749,15	2,50	0,237
Residual error	12	3596,3	299,69		0,570
Total	17	6306,7			

According to *Fz(N)*

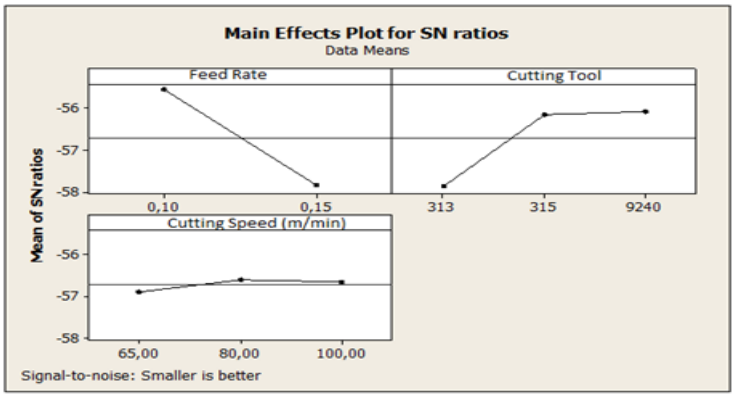

Fig. 3. Mean response graphs of the cutting forces according to feed rate, cutting speed and cutting tool According to *Ra* (μm)

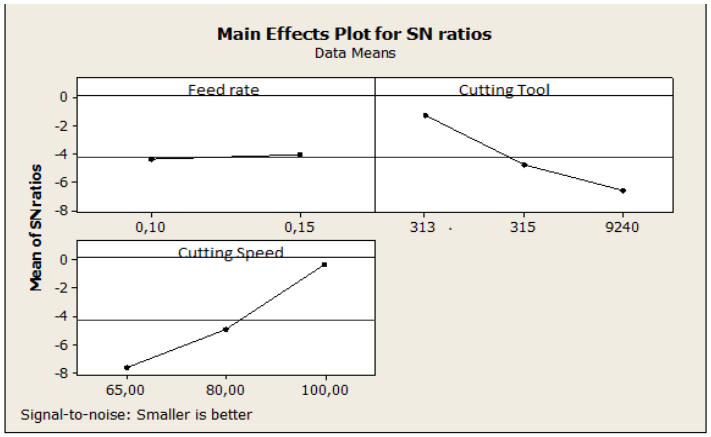

Fig. 4 Mean response graphs of surface roughness according to feed rate, cutting speed and cutting tool

Table 9 Results of confirmation tests for Cutting force (N)

	Starting cutting parameters	Optimal cutting parameters	
		Prediction	Experimental
Level	A1B1C2	A1B2C2	A1B2C2
Cutting force (N)	505	453,5	550
S/N ratio (dB)	-54,0658	-54,0374	-57,8072
Improvement of S/N ratio	3,7414dB		
Prediction error (dB)	3,7698		

Table 10 Results of confirmation tests for surface roughness, Ra (μm)

	Starting cutting parameters	Optimal cutting parameters	
		Prediction	Experimental
Level	A1B2C3	A1B1C3	A1B1C3
Cutting force (N)	1,027	11,7149	0,725
S/N ratio (dB)	-0,2314	-233,656	-2,7932
Improvement of S/N ratio	2,5618 dB		
Prediction error (dB)	230,8628		

CONCLUSIONS

The experimental design described herein was used to develop a main cutting force and surface roughness prediction model roughness using analysis of Taguchi for turning Inconel 625. Results of this experimental study can be summarized as follows:

• Taguchi orthogonal array arrangement, it has seen appropriate to analyzed the cutting force and average surface roughness defined in this article.

• According to ANOVA results. The effect of cutting tool on cutting force was obtained as 398 % and the effect of cutting speed on average surface roughness was obtained 237 % as in high levels.

• According to turning test results, the depth of cut and feed rate are two main parameters between four can be controlled factor (cutting tool, cutting speed, feed rate, depth of cut) affecting average surface roughness and cutting forces. While cutting speed and cutting tool has higher effect on the cutting force, the cutting tool and cutting speed has higher effect on the average surface roughness it has seen in this experiments on machining Inconel 625.

•It was obtained better cutting force and surface roughness at almost the same level of the testing range with the parameters listed in machining Inconel 625,

•Maximum main cutting force 887N was found with uncoated cemented carbide inserts.

•Minimum average surface roughness (0.812μm) is determined with K313 CNMG 120404MS uncoated carbide tools and maximum average surface roughness (4.785μm) is observed with CNMG 120404FN type multicoated PVD (TIN, TICN, TIN, WC) carbide tools

ACKNOWLEDGEMENTS

The authors would like to express their gratitude to University of Yuzuncu Yıl for the financial support Under Project No. BAP-MYO-2012

REFERENCES

[1]. P. Ganesan, C.M. Renteria, J.R. Crum, Verstile corrosion resistance of Inconel 625 in various aqueous and chemical processing environments, TMSPittsburgh,Pennsylvania, USA, 1991.
[2]. Special Metals Corporation Products, INCONEL® alloy 625, www.specialmetals.com/products.
[3]. H. Bohm, K. Ehrlich, K.H. Kramer, Metall 24 (1970) 139–144.
[4]. H.K. Kohl, K. Peng, J. Nucl. Mater. 101 (1981) 243–250.
[5]. W.E. Quist, R. Taggart, D.G. Polonis, Metall. Trans. 2 (1971) 825–832.
[6]. M. Sundararaman, P. Mukhopadhyay, S. Banerjee, Met. Trans. A19 (1988) 453–465.
[7]. T. Charles, Int. J. Press. Vessels Piping 59 (1994) 41–49.
[8]. V. Shankar, K. Bhanu Sankar Rao, S.L. Mannan, J. Nucl. Mater. 288 (2001) 222–232.
[9]. L.E. Shoemaker, in: E.A. Loria (Ed.), Superalloys 718, 625, 706 and Various Derivatives, TMS,Warrendale, PA, 2005, pp. 409–418.
[10]. G.H. Gessinger, Powder Metallurgy of Superalloys, Butterworth & Co., London, 1984, pp. 3–15.
[11]. J.J. Valencia, J. Spirko, R. Schmees, in: E.A. Loria (Ed.), Superalloys 718, 625, 706 and Various Derivates, TMS,Warrendale, PA, 1997, pp. 753–762.
[12]. S. Sun, M. Brandt, M.S. Dargusch, Characteristics of cutting forces and chi formation in machining of titanium alloys, International Journal of Machine Tools and Manufacture 49 (2009) 561–568.
[13]. S. Ranganath, A.B. Campbell, D.W. Gorkiewicz, A model to calibrate and predict forces in machining with honed cutting tools or inserts, International Journal of Machine Tools & Manufacture 47 (2007) 820–840.
[14]. E.S. Topal, C. Cogun, A cutting force induced error elimination method for turning operations, Journal of Materials Processing Technology 170 (2005) 192–203.

[15]. F.A. Almeida, F.J. Oliveira, M. Sousa, A.J.S. Fernandes, J. Sacramento, R.F. Silva Machining hardmetal with CVD diamond direct coated ceramic tools: effect of tool edge geometry, Diamond & Related Materials 14 (2005) 651–656.
[16]. G. Byrne, D. Dornfeld, I. Inasaki, G. Ketteler, W. Konig, R. Teti, Tool condition monitoring (TCM)—the status of research and industrial application, Annals of the CIRP 44/2 (1995) 541–567.
[17]. J. Tlusty, G.C. Andrews, A critical review of sensors for unmanned machining,Annals of the CIRP 32/2 (1983) 563–572.
[18]. A. Kirchheim, J. Stirnimann, D. Veselovac, H^3 high performance, high accuracy and high frequency. In: Proceedings of the CIRP 2nd International Conference,
High Performance Cutting (HPC), 12–13 June 2006, Vancouver, Canada
[19]. C. Scheffer, P.S. Heyns, An industrial tool wear monitoring systems for interrupted turning, Mechanical Systems and Signal Processing 18 (2004)
1219–1242.
[20]. J. Gradisek, E. Govekar, I. Grabec, Using coarse-grained entropy rate to detect chatter in cutting, Journal of Sound and Vibration 214 (5) (1998) 830–841.
[21]. S. Tangjitsitcharoen, In-process monitoring and detection of chip formation and chatter for CNC turning, Journal of Materials Processing Technology 209 (2009) 4682–4688
[22]. K. Palanikumar, Experimental investigation and optimisation in drilling of GFRP composites, Measurement 44 (2011) 2138–2148.
[23]. J.P. Davim, P. Reis, Machinability study on composite (Polyetheretherketone reinforced with 30% of glass fiber-PEEK GF
30) using polycrystalline diamond (PCD) and cemented carbide (K20) tools, International Journal of Advanced Manufacturing Technology 23 (2004) 412–418.
[24]. S. Yaldız, F. Ünsaçar, Design, development and testing of a turning dynamometer for cutting force measurement, Materials and Design 27–10 (2006) 839–846
[25]. K. Palanikumar, J.P. Davim, Assessment of some factors influencing tool wear on the machining of glass fibre-reinforced plastics by coated cemented carbide tools, Journal of Materials Processing Technology 209 (2009) 511–519.
[26]. J.P. Davim, A.P. Monteiro Baptista, Relationship between cutting force and PC cutting tool in machining silicon carbide reinforced aluminium, Journal of Materials Processing Technology 100–3 (2000) 417–423.
[27]. J.P. Davim, Diamond tool performance in machining metal–matrix composites Journal of Materials Processing Technology 128 (2002) 100–105
[28]. W. Konig, A. Berktold, J. Liermann, N. Winands, Top quality components not only by grinding. *Ind. Diamond Rev.* 3 (1994), pp. 127–132.
[29]. Taskesen A, Kütükde K, Optimization of the Drilling Parameters for The Cutting Forces in B4C-Reinforced AL-7XXX- Series Alloys Based On The Taguchi Method Materiali in Technologie MTAEC9, 47(2)169(2013)
[30]. G. Tosun, Statistical analysis of process parameters in drilling of AL/SIC P metal matrix composite, International Journal of Advanced Manufacturing Technology, 55 (2011) 5–8, 477–485
[31]. R. K. Roy, A primer on the Taguchi method / Ranjit K. Roy, Van Nostrand Reinhold, New York, (1990)